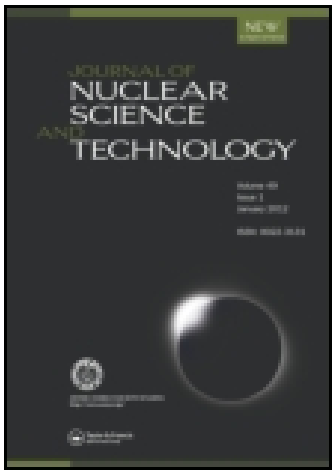

Journal of Nuclear Science and Technology
Publication details, including instructions for authors and subscription information:
http://www.tandfonline.com/loi/tnst20

Shielding study at the Fukui Prefectural Hospital Proton Therapy Center

Daiki Satoh [a] , Yoshikazu Maeda [b] , Yuji Tameshige [b] , Hiroshi Nakashima [a] , Tokushi Shibata [a] , Akira Endo [a] , Shuichi Tsuda [a] , Makoto Sasaki [b] , Motokazu Maekawa [b] , Yasuhiro Shimizu [b] , Masaharu Yamazaki [c] , Tadashi Katayose [c] & Koji Niita [d]

[a] Japan Atomic Energy Agency, Tokai-mura, Naka-gun , Ibaraki , 319-1195 , Japan

[b] Fukui Prefectural Government, Yotsui, Fukui-shi , Fukui , 910-8526 , Japan

[c] Mitsubishi Electric Corporation, Marunouchi, Chiyoda-ku , Tokyo , 100-8310 , Japan

[d] Research Organization for Information Science and Technology, Tokai-mura, Naka-gun , Ibaraki , 319-1195 , Japan

Published online: 23 Oct 2012.

To cite this article: Daiki Satoh , Yoshikazu Maeda , Yuji Tameshige , Hiroshi Nakashima , Tokushi Shibata , Akira Endo , Shuichi Tsuda , Makoto Sasaki , Motokazu Maekawa , Yasuhiro Shimizu , Masaharu Yamazaki , Tadashi Katayose & Koji Niita (2012) Shielding study at the Fukui Prefectural Hospital Proton Therapy Center, Journal of Nuclear Science and Technology, 49:11, 1097-1109, DOI: 10.1080/00223131.2012.730900

To link to this article: http://dx.doi.org/10.1080/00223131.2012.730900

Journal of Nuclear Science and Technology
Volume 49, No. 11, November (2012) pp. 1097–1109
http://www.tandfonline.com

ARTICLE

Shielding study at the Fukui Prefectural Hospital Proton Therapy Center

Daiki Satoh[a]*, Yoshikazu Maeda[b], Yuji Tameshige[b], Hiroshi Nakashima[a], Tokushi Shibata[a†], Akira Endo[a], Shuichi Tsuda[a], Makoto Sasaki[b], Motokazu Maekawa[b], Yasuhiro Shimizu[b], Masaharu Yamazaki[c], Tadashi Katayose[c] and Koji Niita[d]

[a]*Japan Atomic Energy Agency, Tokai-mura, Naka-gun, Ibaraki 319-1195, Japan;* [b]*Fukui Prefectural Government, Yotsui, Fukui-shi, Fukui 910-8526, Japan;* [c]*Mitsubishi Electric Corporation, Marunouchi, Chiyoda-ku, Tokyo 100-8310, Japan;* [d]*Research Organization for Information Science and Technology, Tokai-mura, Naka-gun, Ibaraki 319-1195, Japan*

(*Received 13 June 2012; accepted final version for publication 9 September 2012*)

At the Fukui Prefectural Hospital Proton Therapy Center, neutron doses behind the concrete shields and at the maze were measured with three types of radiation monitors (DARWIN, Wendi-2, and a rem meter) along with solid-state nuclear track detectors. The measured data were compared with estimations of analytical models and the Monte Carlo code, Particle and Heavy-Ion Transport code System (PHITS). The analytical model, using the parameters employed in the shielding design of the facility, gave considerably larger values than the measured data. This means that the facility was designed with a sufficient margin of safety. The results calculated by PHITS were less than those of the analytical model and were about three times larger than the measured data. From a perspective that seeks conservative estimation with less margin, the Monte Carlo simulation is a good tool for shielding design of accelerator-based proton treatment facilities.

Keywords: proton therapy; shielding design; dose measurement; analytical model; Monte Carlo code; PHITS; bulk shielding; maze; neutron; photon

1. Introduction

In the last decade, charged particle radiotherapy using protons or heavier ions has made remarkable progress as an advanced medical treatment against cancer because of its clinical advantages over conventional radiation therapy with X-rays or electrons. The physical properties of protons and heavier ions, whereby dose is largely deposited in the narrow Bragg peak at a fixed depth in tissue, provide clinicians with a good tool to sharply conform the radiation field around the tumor while reducing unnecessary irradiation to normal tissue. As of January 2012, about 30 proton treatment facilities are in operation worldwide, and 21 facilities are either being planned or are under construction [1]. The charged particle beams used in the therapy require kinetic energies of a few hundred mega-electron volts. A typical facility for charged particle radiotherapy might be an accelerator cascade, which consists of an injector, a cyclotron or a synchrotron to accelerate the charged particles to the therapeutic energy, beam transport lines, and several treatment rooms. At these facilities, various kinds of secondary radiation are produced during treatment when the accelerated particles interact at a nuclear level with the materials composing the accelerator and the beam transport lines. Moreover, a patient treated with the accelerated particles becomes a source of the secondary radiation because incident charged particles lose almost all kinetic energy and stop in the patient's body. To protect people in the facility and the public from undesirable exposures to the secondary radiation, the facility must be equipped with proper shielding that attenuates the radiation to acceptable levels.

The secondary radiation is usually attenuated as it passes through a thick wall, called bulk shielding. Outside a thick shield, neutrons become a main component of the radiation due to their strong penetrability against shielding materials. Energies of these neutrons range wide, that is, from thermal energy to the incident beam energy. The high-energy neutrons are produced via spallation reactions and pass through the shielding without much energy degradation. The low-energy ones are produced by the interactions of high-energy neutrons, and come from inside the shield.

*Corresponding author. Email: satoh.daiki@jaea.go.jp
†Present address: Chiyoda Technol Corporation, Oarai-machi, Higashiibaraki-gun, Ibaraki 311–1313, Japan.

ISSN 0022-3131 print/ISSN 1881-1248 online

http://dx.doi.org/10.1080/00223131.2012.730900

Photons are also generated inside the shield as a result of thermal neutron capture and inelastic reactions. Secondary charged particles would be blocked by shielding designed for neutrons since the attenuation length is shorter than that of neutrons. In addition to the bulk shielding, mazes are often used to weaken radiation field, instead of a massively shielded door at treatment room entrances. A maze is a passage that connects the entrance and the shielded room and consists of multiple legs, which are normally perpendicular to each other, to avoid the direct propagation of radiation to the entrance. Proper shielding design not only ensures radiation safety but also lowers construction costs.

Analytical models [2,3] described by a simple equation have conventionally been used to design bulk shielding and mazes. The advantages of analytical models are of a practical nature: they are convenient to use and provide rapid, inexpensive dose estimations. The disadvantages are that they require quite simplistic assumptions and depend strongly on parameters, which restrict their applicability and degrade their accuracy under complicated situations. On the other hand, shielding design based on a Monte Carlo code has become an attractive choice with the advent of powerful computers. It can provide a map of dose distribution in the facility at once by a simulation of radiation transport in a three-dimensional geometry that models the actual structure of a facility. In fact, the results of Monte Carlo codes such as PHITS [4], MCNPX [5], FLUKA [6], and GEANT4 [7] have been employed in the design of either part or all of the shielding at several accelerator facilities [8–10].

In this article, we report the results of neutron dose measurements at the Fukui Prefectural Hospital Proton Therapy Center, which is a proton treatment facility in the Fukui Prefecture, Japan. The neutron doses were measured behind shields of a treatment room in forward and perpendicular directions by use of several radiation monitors of DARWIN [11,12], Wendi-2 [13,14], and rem meter [15]. The neutron dose distribution in a maze was also obtained by solid-state nuclear track detectors [16]. The experimental results were compared with the predictions of the analytical models and the PHITS code to investigate the reliability of their design calculations for shielding at the proton treatment facility.

2. Radiation safety design of the Fukui Prefectural Hospital Proton Therapy Center

The Fukui Prefectural Hospital Proton Therapy Center is a three-story building next to the main hospital building. **Figure 1** shows a bird's eye perspective of the first floor, dedicated mainly to the proton therapy facility. The accelerator cascade is composed of a 7-MeV-injector linac and a compact synchrotron that supplies proton beam energies of 70–235 MeV with a maximum beam current of 11 nA. Accelerated protons are slowly extracted from the synchrotron as pulsed output typically 0.4 s long and with a repetition rate of 0.5 Hz. Then proton beams are transported by a

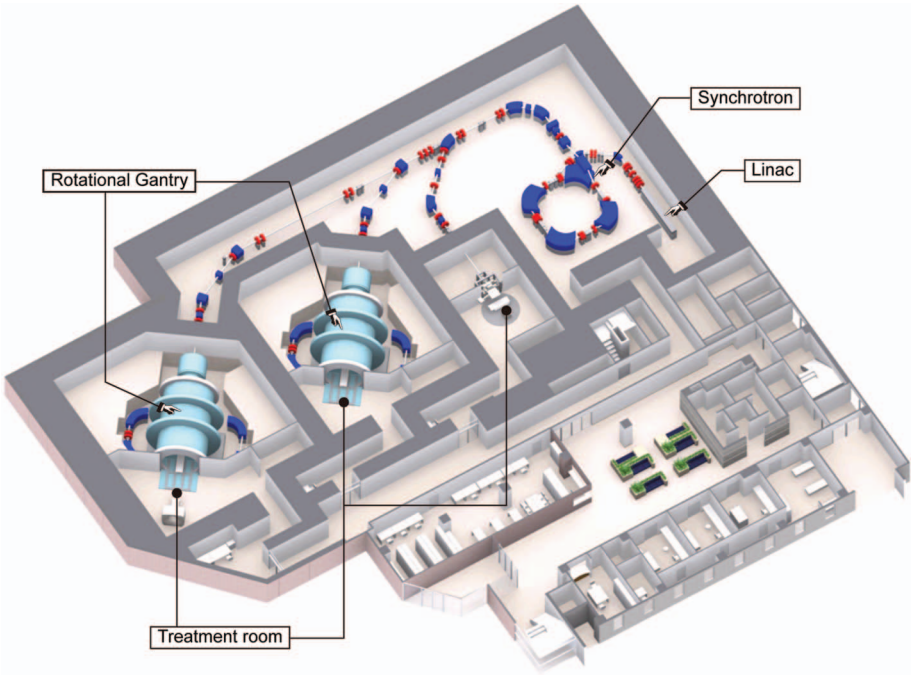

Figure 1. Layout of the Fukui Prefectural Hospital Proton Therapy Center. The installation has a synchrotron, a fixed beam room, and two gantry rooms.

series of dipole and quadrupole magnets to three treatment rooms. Two of them are equipped with rotating gantries, and the other uses a horizontal fixed beam. The broad-beam method, with a couple of wobbling electromagnets and a scatterer plate, has been adopted because of its efficacy for forming the irradiation field.

The radiation safety design was performed with the analytical models and the parameters described in the next section, which have generally been employed in the construction of proton treatment facilities in Japan. The equipment is shielded with ordinary concrete of 2.2 g/cm^3 density, and plates of steel are also used as additional shielding material. The values of the beam losses along the beam transport used in the design planning were provided by the equipment vendor, Mitsubishi Electric Corporation [2]. **Table 1** summarizes the maximum values of effective dose rate calculated at the boundaries of the radiation controlled area and the facility site, together with the dose limits given in the Japanese regulations for radiation protection. According to the estimated value in the planning, the facility is properly designed to satisfy the legal dose limits.

The Fukui Prefectural Hospital Proton Therapy Center was constructed in 2010 in accordance with its radiation safety application and the admission procedures established by the Japanese Government, and has been in operation for radiotherapy since March 2011. Over 100 patients were treated in the first year.

3. Analytical models

3.1. Bulk shielding

The bulk shielding of the Proton Therapy Center was estimated by using an analytical model [2] expressed in the following equation that combines an inverse square law, a room scattering correction, and an exponential attenuation through the shield:

$$H = \frac{H_0(\theta)}{r^2} \cdot J \cdot \left[1 + \frac{(f-1)r'^2}{R^2}\right] \cdot \exp\left(-\frac{d}{\lambda(\theta)}\right) \quad (1)$$

where H is the effective dose outside the shield; $H_0(\theta)$ indicates the source term, that is, the dose per unit beam loss at 1 cm away from the source along a production angle θ with respect to the incident beam axis; r is the distance between the source and the scoring points; J is the beam loss; f is the correction factor of backscattering inside the room; r' is the distance from the source point to the shielding wall; R is the radius of a sphere that has the identical surface area as the room; d is the thickness of the wall; and $\lambda(\theta)$ denotes the attenuation length in the shield for neutrons produced at angle θ.

Table 1. Maximum dose rates (μSv/3 months) at each area boundary estimated in design planning.

Boundary	Estimation	Dose limit
Controlled area	1,101	1,300
Facility site	196	250

The source term was estimated from the experimental data [17] of neutron production by 256-MeV protons bombarding upon thick targets measured at Los Alamos National Laboratory (LANL). Note that the incident energy of the LANL data is 256 MeV, while the therapeutic energy at the facility is 235 MeV. In addition, since the experimental data exist only at angles greater than 7.5°, the neutron doses at forward angles less than 7.5° were estimated by doubling the results calculated with the parameters at 7.5° [2].

The attenuation length for concrete and the correction factor for the room scattering effect were calculated by a one-dimensional discrete ordinates transport code ANISN [18] in combination with DLC-119/HILO86 multi-group cross-section library [19]. **Figure 2** depicts the one-dimensional spherical geometry used in the ANISN calculation. A point source of neutrons is located at the center of the sphere with the energy spectrum based on the LANL data. The distance between the source and concrete wall is 400 cm, and the thickness of the wall is set to 200 cm. The attenuation curves were obtained from the calculated dose distributions in the shielding. The correction factors for room scattering effect were evaluated by comparing two neutron spectra in front of the shield: one is derived by attenuating the source neutron spectrum with an inverse square law, and the other is calculated by ANISN. The factor f varies from

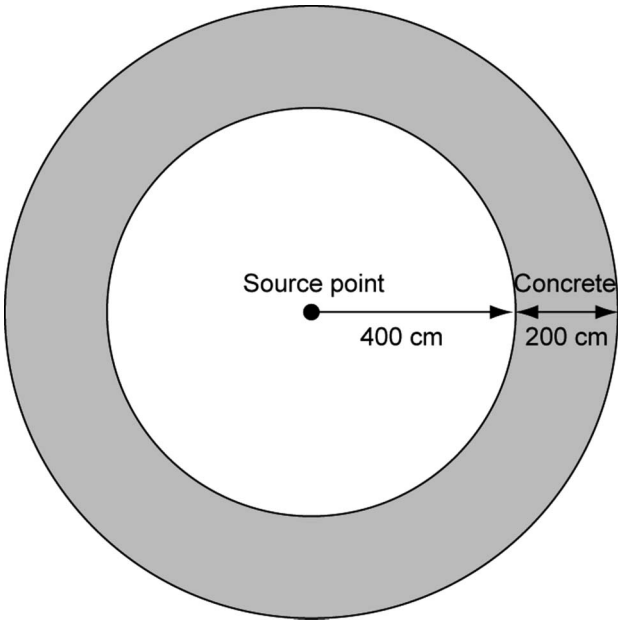

Figure 2. One-dimensional spherical geometry in ANISN calculation.

2 to 3.5 depending on the emission angles and the target materials [2].

3.2. Maze

Analytical formulas proposed by Nakamura and Uwamino [3] were applied to the design of multi-leg mazes. The effective dose $H(r)$ at the mouth of the first leg is predicted with

$$H(r) = D_0\left(\frac{1}{r^2} + \frac{a}{r^2 + 4s^2 - 2\sqrt{2}rs}\cdot\frac{A'}{A}\right), \quad s = \frac{\sqrt{L_1 L_2}}{2} \tag{2}$$

where r is the distance between a point source and the maze mouth; D_0 is the effective dose at 100 cm away from the source; a is the adjustable parameter; L_1 and L_2 denote the diameter and length of a cylinder, respectively, whose volume is equivalent to that of the actual room; A is the total surface area of the room; and A' is the surface area of the room seen directly from the mouth of the first leg. The first and second terms in Equation (2) are the contributions of the direct and the scattered radiations obeying an inverse square law. In the design planning for the Fukui Prefectural Hospital Proton Therapy Center, the parameters were set as $a = 4$ and $A'/A = 1$ to keep the estimations conservative.

The neutron dose in the ith leg $H(r_i)$ is estimated by attenuating the dose at a pseudo source $H(a)$ with an inverse square law as the following:

$$H(r_i) = H(a)\frac{a^2}{{r_i}^2}, \tag{3}$$

where a is half the narrower size between width and height of the cross section of the leg, and r_i is the distance between the pseudo source and the scoring point. The pseudo source is located in the preceding leg at a distance a away from the mouth of ith leg.

4. Monte Carlo code

Particle and Heavy-Ion Transport code System (PHITS) [4] is employed as a Monte Carlo code to examine the applicability of shielding calculations at a proton treatment facility. The PHITS is a multi-purpose Monte Carlo code to deal with the transport and reaction of all particles (nucleons, nuclei, mesons, photons, and electrons) over wide energy ranges using theoretical models and nuclear data files.

A three-dimensional geometry for the PHITS calculation was constructed according to the Computer Aided Design (CAD) data of the actual facility as shown in **Figure 3**. The sources of radiation were set at beam-loss points of the injection and extraction septum magnets, at the beam shaping device, and at the beam stops [2]. **Figure 4** depicts the map of neutron dose distribution calculated under the conditions almost equivalent to those in the analytical calculation. The proton beam current is 10 nA, the operation time of the accelerator is 18.0 h/week, and the irradiation time at each treatment room is 3.8 h/week. Note that the beam is supplied at the rotating gantry rooms with the incident angles of 0°, 45°, 90°, and 270°, equally. The dotted and bold lines indicate the boundaries of the radiation controlled area and the facility site, respectively. As shown in the figure, PHITS can give the dose rate at any location in the facility with a single calculation that considers particle transport in a complex geometry, and we can judge whether or not the calculated values satisfy the legal dose limits. This use of a Monte Carlo code is a very powerful feature in shielding design.

5. Measurements

5.1. Experimental conditions

The schematics of the experimental setup, showing horizontal (upper) and vertical (lower) sections, are shown in **Figure 5**. The 235-MeV protons were extracted from the synchrotron and were transported to the horizontal fixed beam room without adapting wobbling magnets or scatterer. The current of the beam was set to 10 nA and was monitored during the experiment by ionization chambers equipped in the irradiation-field formation system. The output of the ionization chambers was connected to a current integrator and was calibrated with a Faraday cup to deduce the beam current. The uncertainty of the beam current estimates was found to be below 10%. The beam stopped in a water phantom mounted on a bed for patients in the treatment room. The phantom consisted of pure water filled in a 1-cm-thick acrylic resin container that measured 25 cm by 25 cm on the front face and 40 cm in depth.

The radiation monitors, DARWIN, Wendi-2, and a rem meter, were located behind the concrete shields of 385 and 250 cm thickness in the forward and perpendicular (overhead) directions, respectively. The solid-state nuclear track detectors were fixed with strings along the centerlines on a floor and a ceiling in the maze. These detectors gave the neutron dose distribution in the maze at seven locations.

5.2. Radiation monitors

5.2.1. DARWIN

The DARWIN is a dose and spectrum monitoring system developed at Japan Atomic Energy Agency [11,12]. It can output not only radiation dose but also energy spectrum. **Figure 6** shows an overview of the DARWIN system, which is composed of (a) a phoswich-type detector consisting of a liquid organic scintillator (12.4 cm in diameter and 12.7 cm thick) coupled with ZnS(Ag) scintillation sheets doped with ^{6}Li, (b) a data-acquisition module for digital waveform analysis of the detector signals, and (c) a personal

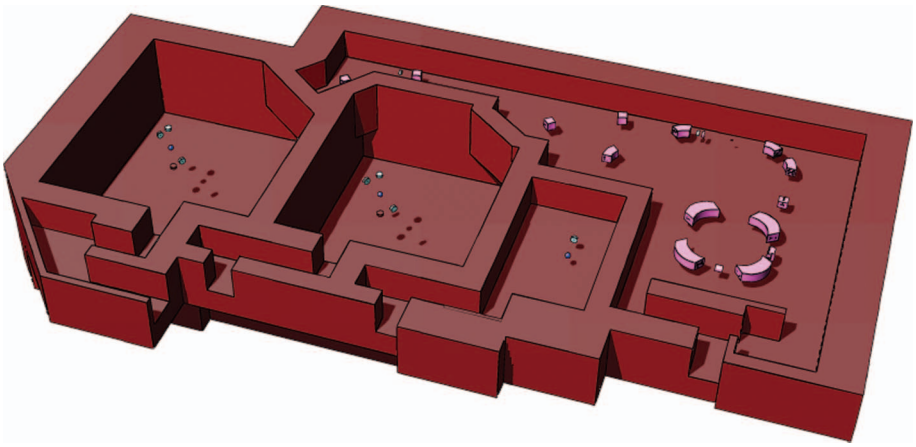

Figure 3. Three-dimensional geometry of the Fukui Prefectural Hospital Proton Therapy Center modeled in PHITS.

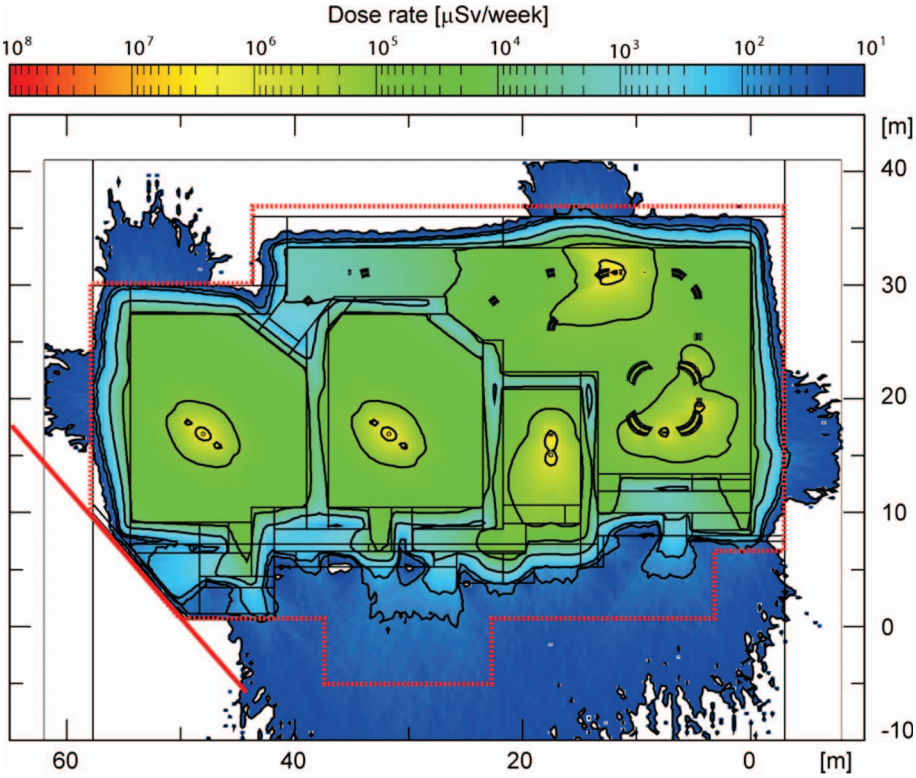

Figure 4. Map of neutron dose rate distribution calculated by PHITS. The dotted and bold lines represent the boundaries of the controlled area and the facility, respectively.

computer for controlling the system and visualizing the measured data. The total weight of the system is less than 10 kg.

The DARWIN is applicable to dose measurement of neutrons, photons, and muons with energy ranges between thermal energy and 1 GeV, 150 keV and 100 MeV, and 1 MeV and 100 GeV, respectively. Each type of radiation is distinguished from the others according to its waveform by use of the pulse-shape and height discrimination technique [11]. The doses are estimated on the basis of a G-function method [20,21], and the energy spectra are deduced by an unfolding method [22,23]. By post-analysis of the waveforms saved event by event, DARWIN outputs the doses of both ambient dose equivalent H*(10) and effective dose for Antero-Posterior (AP) irradiation. The performance of DARWIN had been validated in several calibration fields [11,12]. In the present experiment, a background measurement was also performed to estimate the contributions of cosmic rays.

5.2.2. *Wendi-2*

The Wendi-2 is a wide-range neutron detector originally developed at LANL and commercialized by Thermo Scientific [13,14]. An overview of Wendi-2

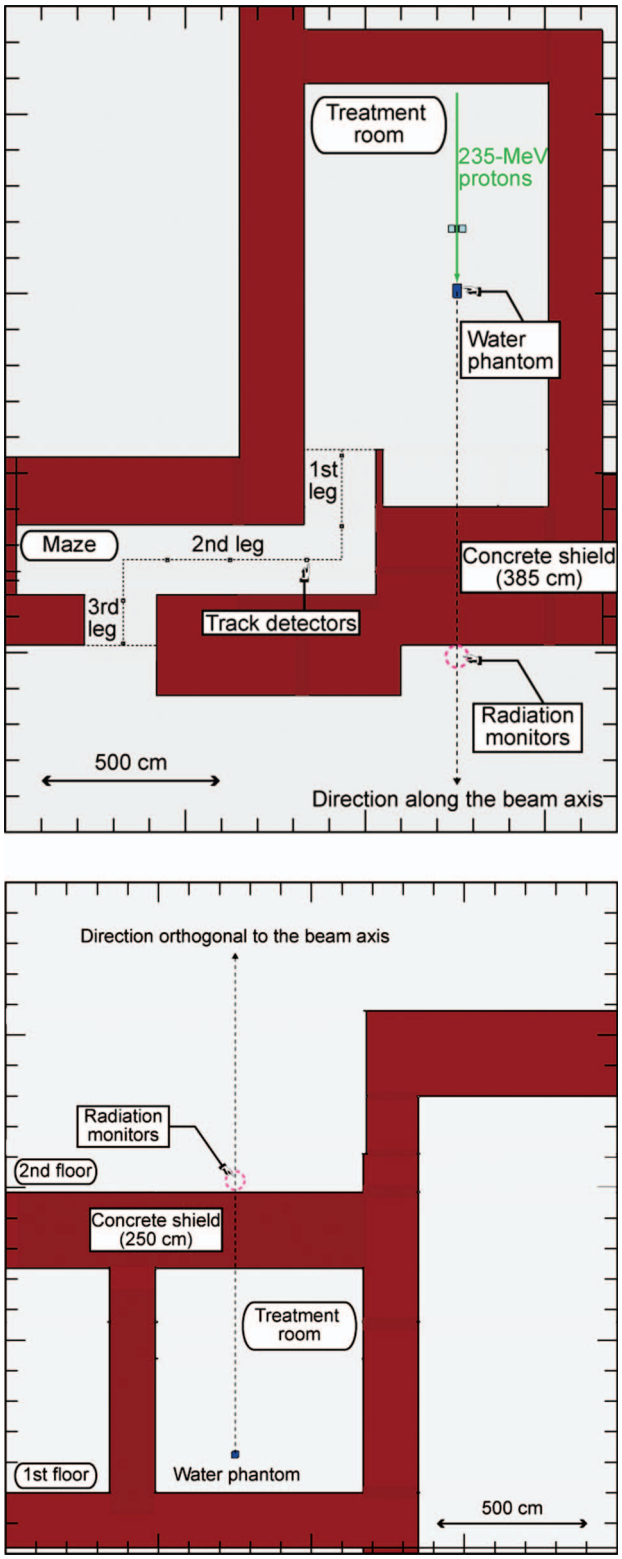

Figure 5. Experimental setup at the horizontal fixed beam room with horizontal (upper) and vertical (lower) section views.

is shown in **Figure 7**. A ^{3}He proportional counter is positioned in the center of a cylindrical polyethylene moderator assembly, and a tungsten powder shell is embedded around the counter to improve the response for high-energy neutrons. Wendi-2 weighs 13.5 kg.

The geometrical design of Wendi-2 makes its energy response follow the contour of the ambient dose equivalent per unit fluence function H*(10)/Φ. The applicable energy range is from 25 meV to 5 GeV according to the dose-conversion coefficients listed in Publication 74 [24] of the International Commission on Radiological Protection (ICRP) for an energy range between 25 meV and 180 MeV and supplemented by the calculations [25] of Sannikov and Savitskaya for an energy range between 300 MeV and 5 GeV.

The output signal of Wendi-2 was processed with a specialized unit manufactured by Thermo Scientific. The unit also connected with a personal computer and stored the dose data with digital time stamps.

5.2.3. *Rem meter*

An ordinary rem meter, the Wedholm Medical 2222A [15] shown in Figure 7, was also used as a neutron monitor. It consists of a BF_3 proportional counter surrounded by polyethylene and a boron moderator assembly. The energy response for the ambient dose equivalent H*(10) corresponds with the reference curve given by the ICRP [24], but the applicable energy is restricted below 17 MeV because ordinary rem meters lack sensitivity to high-energy neutrons.

The pulses outputted from the rem meter were fed into a NIM scaler. The neutron dose rate was derived by applying a dose-conversion factor calibrated with an AmBe source to the number of pulses counted by the scaler.

5.2.4. *Solid-state nuclear track detector*

Solid-state nuclear track detectors were used to measure the neutron dose distribution in the maze. The track detector, manufactured by Chiyoda Technol Corporation, is made of a poly-allyl diglycol carbonate (PADC) plastic, often referred to as CR-39 [16]. Neutrons of a wide energy range are detected through nuclear reactions of H(n,p) for fast neutrons and ^{10}B(n, α)^{7}Li on a boron nitride converter for thermal ones. The energy dependence of the detector response is calibrated in free air to follow the conversion coefficients from neutron fluence to the ambient dose equivalent H*(10) defined by ICRP [24].

The etch pits on the PADC caused by the nuclear reactions were analyzed offline, which gave the cumulative dose during the exposure. The applicable energy is restricted up to about 15 MeV, because higher energy neutrons that penetrate the PADC deposit only a small amount of energy, making no clearly visible etch pits.

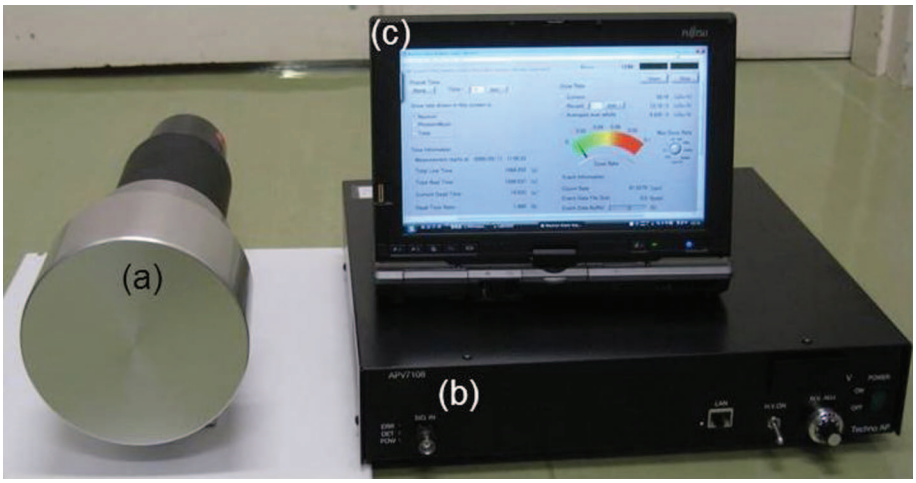

Figure 6. Overview of the DARWIN system that consists of (a) a phoswich-type detector, (b) a data-acquisition module, and (c) a personal computer.

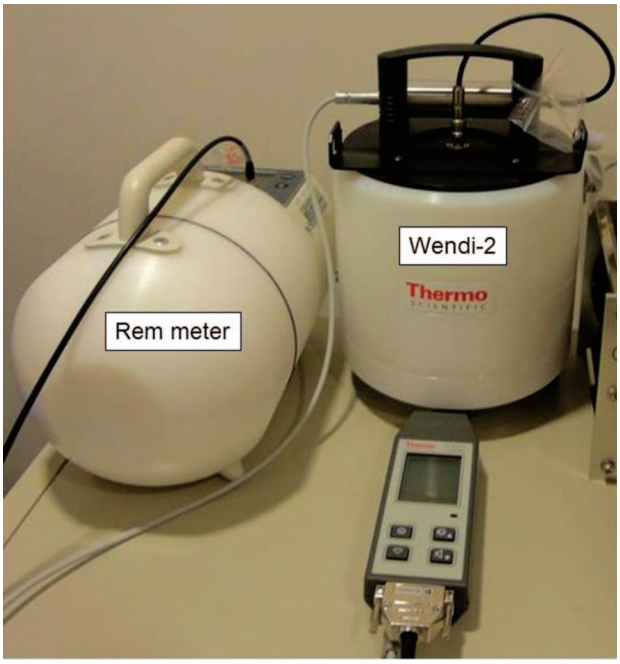

Figure 7. Wendi-2 (FHT 762) with dose rate measuring unit (FH 40 G) manufactured by Thermo Scientific (right) and a rem meter (2222A) manufactured by Wedholm Medical (left).

6. Results and discussions

6.1. Bulk shielding

6.1.1. Results

Neutron dose rates measured by the radiation monitors behind the concrete shields are summarized in **Table 2** together with the results of PHITS and the analytical model. Here, the forward and overhead directions are referred to as 0° and 90°, respectively. The data from the rem meter at 90° were below the detection limit. The PHITS results were calculated with the high-energy nuclear data file JENDL/HE-2007 [26] for neutrons and protons. The parenthesized PHITS result indicates the value calculated for neutrons below 17 MeV, which corresponds to the upper energy limit measured by the rem meter. **Figure 8** depicts the neutron dose rate distribution at the horizontal fixed beam room calculated by the PHITS code.

The results of the analytical model are given in effective dose for AP irradiation, while the others are given in ambient dose equivalent, H*(10). According to the energy spectra measured by DARWIN, the effective dose is about 40% smaller than the ambient dose equivalent under the present experimental conditions.

Table 2. Neutron dose rates behind concrete shields.

Direction (°)	Dose rate (μSv/h)				
	DARWIN	Wendi-2	Rem meter	PHITS	Analytical model
0	1.14	0.86	0.46	3.35 (1.40)[a]	23.4
90	0.099	0.073	–	0.287	5.7

Note: [a]The PHITS data in parentheses is the calculated result for neutrons below 17 MeV.

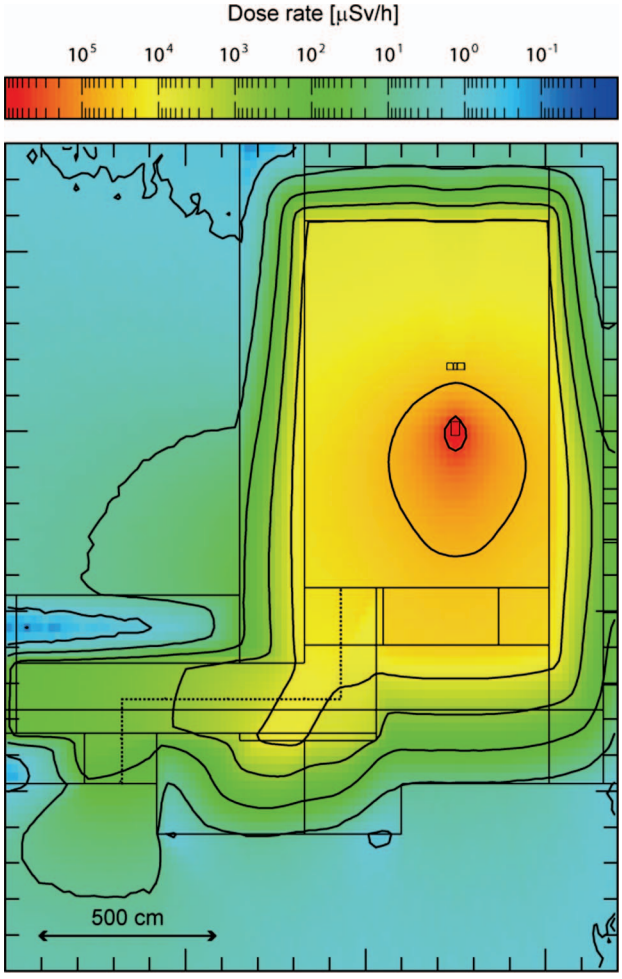

Figure 8. Neutron dose map at horizontal fixed beam room calculated by PHITS.

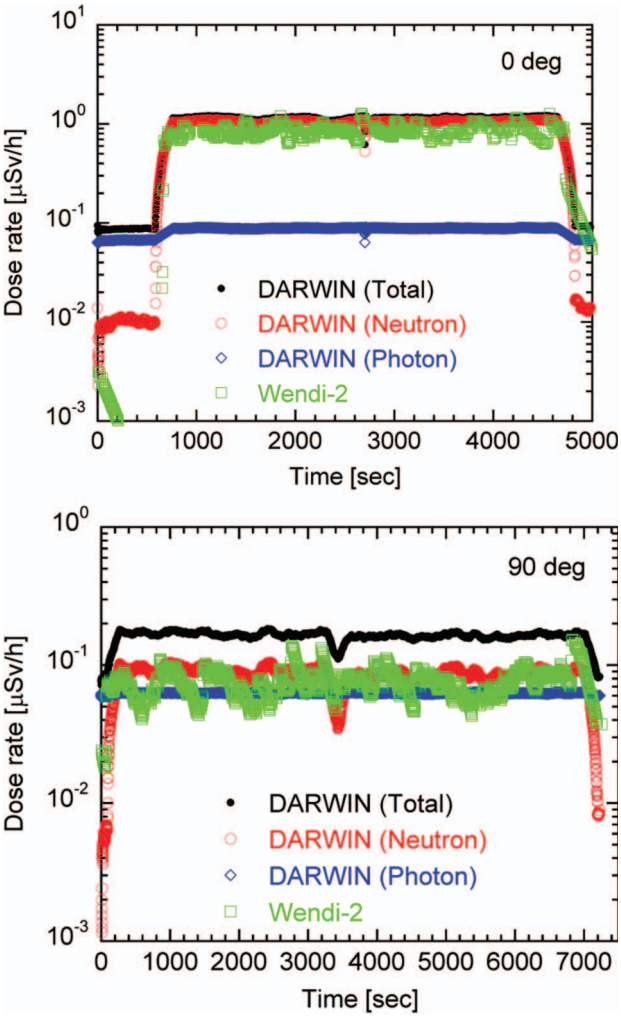

Figure 9. Trends of dose rates measured by DARWIN and Wendi-2 behind shields located in forward (0°, upper) and overhead (90°, lower) directions. Note that the data in each direction were acquired independently, so there is no correlation in the horizontal axes of upper and lower panels.

6.1.2. *Comparison of measured data*

Figure 9 shows the trends of dose rates measured by DARWIN and Wendi-2 during the experiment. The DARWIN and Wendi-2 successfully monitored the fluctuation of dose rates depending on the beam status. The average neutron dose rates of DARWIN are slightly larger than those of Wendi-2 because of the conservative setting of the present G-function. However, both radiation monitors, which have sensitivity to high-energy neutrons, show reasonable agreement.

In the results at 0°, the values of DARWIN are about 2.5 times larger than those of the rem meter. The underestimation of the rem meter comes from the loss of sensitivity for neutrons above 17 MeV. In the PHITS calculation, the ratio of partial dose below 17 MeV to total dose is about 2.4. It should be noted that this value agrees with the ratio of the doses of the rem meter and DARWIN. When using a rem meter to monitor radiation at high-energy accelerator facilities, a neutron dose has conventionally been estimated by doubling the indicated dose value. The present result supports this convention experimentally.

6.1.3. Comparison with analytical calculation

The results of the analytical model with the parameter set used in the design planning are about 20 and 60 times larger for 0° and 90°, respectively, than those of DARWIN as listed in Table 2. The overestimation comes from the overestimation of the source term in Equation (1). The parameter for the source term was determined at a considerable margin of safety. For a more realistic estimation using the model, it is necessary to use the parameters based on experimental data reproducing an actual neutron source in the treatment room.

6.1.4. Comparison with Monte Carlo calculation

Figure 10 shows neutron dose distributions calculated by the Monte Carlo code PHITS through the shields at 0° and 90°, together with the experimental data measured by the radiation monitors behind the shields. The horizontal axis indicates the distance from the center of the water phantom. The PHITS calculations using JENDL/HE yield values about three times larger than the DARWIN experimental data at both 0° and 90°. For the bulk shielding, it was found that the PHITS estimates of neutron dose are between those of DARWIN and the analytical model. From the fact, it is concluded that designing shielding with PHITS is a more realistic option than using analytical models.

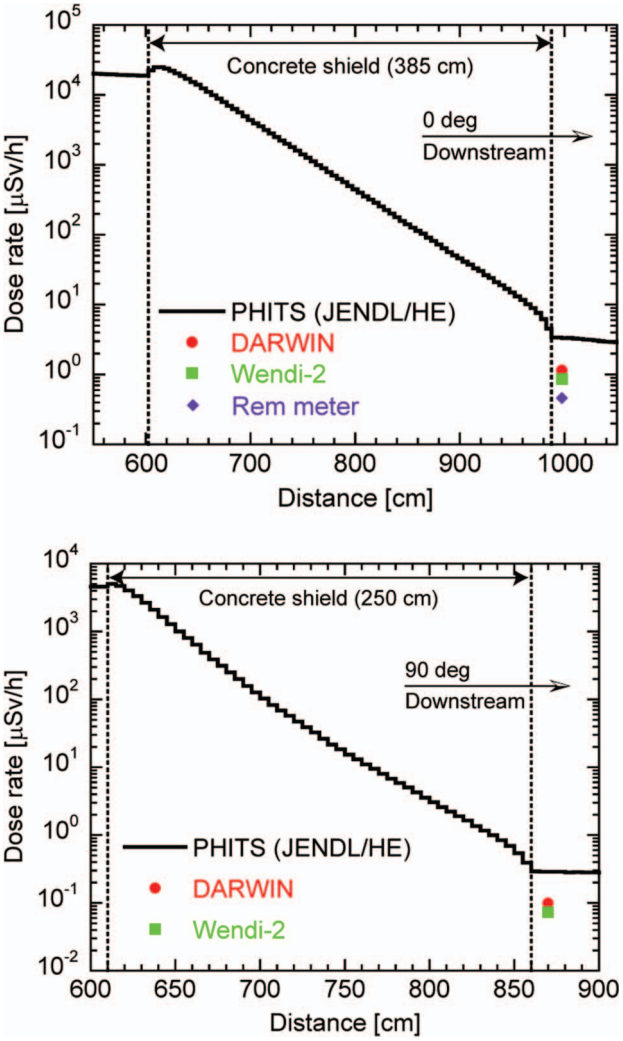

Figure 10. Neutron dose distribution through concrete shields in forward (0°, upper) and overhead (90°, lower) directions. The horizontal axis indicates distance from the center of a water phantom.

Photon dose rates behind the shields are listed in **Table 3**. Note that the results of DARWIN are subtracted the background photon doses by cosmic rays. The calculation results are about 3 and 13 times larger for the 0° and 90° shields, respectively, than those of DARWIN. The deviation at 0° is equivalent to the difference observed in the neutron doses by DARWIN and PHITS. At 90°, however, PHITS shows an overestimation beyond the deviation discussed above. Although the reason has not been verified, photon-production yields in PHITS might be responsible for this problem.

Figure 11 represents the neutron and photon energy spectra behind shields at 0° and 90°. The solid lines indicate the results of DARWIN derived by the unfolding method, and dashed lines are the calculation results of PHITS using JENDL/HE. For neutron spectra, the energy resolution of DARWIN degrades for higher energy neutrons, which penetrate the scintillator, partially impart their energy, and are misidentified in the unfolding process. However, DARWIN and PHITS have similarly shaped neutron spectra. The magnitude of the spectra deviation is equivalent to that observed in the neutron dose measurements. The photon spectra measured by DARWIN is composed of two components: (a) low-energy photons (below 10 MeV) emitted from the capture reaction and de-excitation process of highly excited nuclei and (b) high-energy photons arising from the decay of π^0 mesons, which are created by nucleon–nucleon interactions. On the other hand, the spectra calculated by PHITS with JENDL/HE show continuous distributions. Physical processes emitting photons in hadronic cascade reactions are not incorporated properly into the current JENDL/HE file. To improve the accuracy of the PHITS calculation, the measurements of photon-production double-differential cross sections are under investigation.

Though the PHITS calculations discussed above utilize the nuclear data file, most Monte Carlo codes

Table 3. Photon dose rates behind concrete shields.

Direction (°)	Dose rate (μSv/h)	
	DARWIN	PHITS
0	0.0224	0.0831
90	0.00349	0.0263

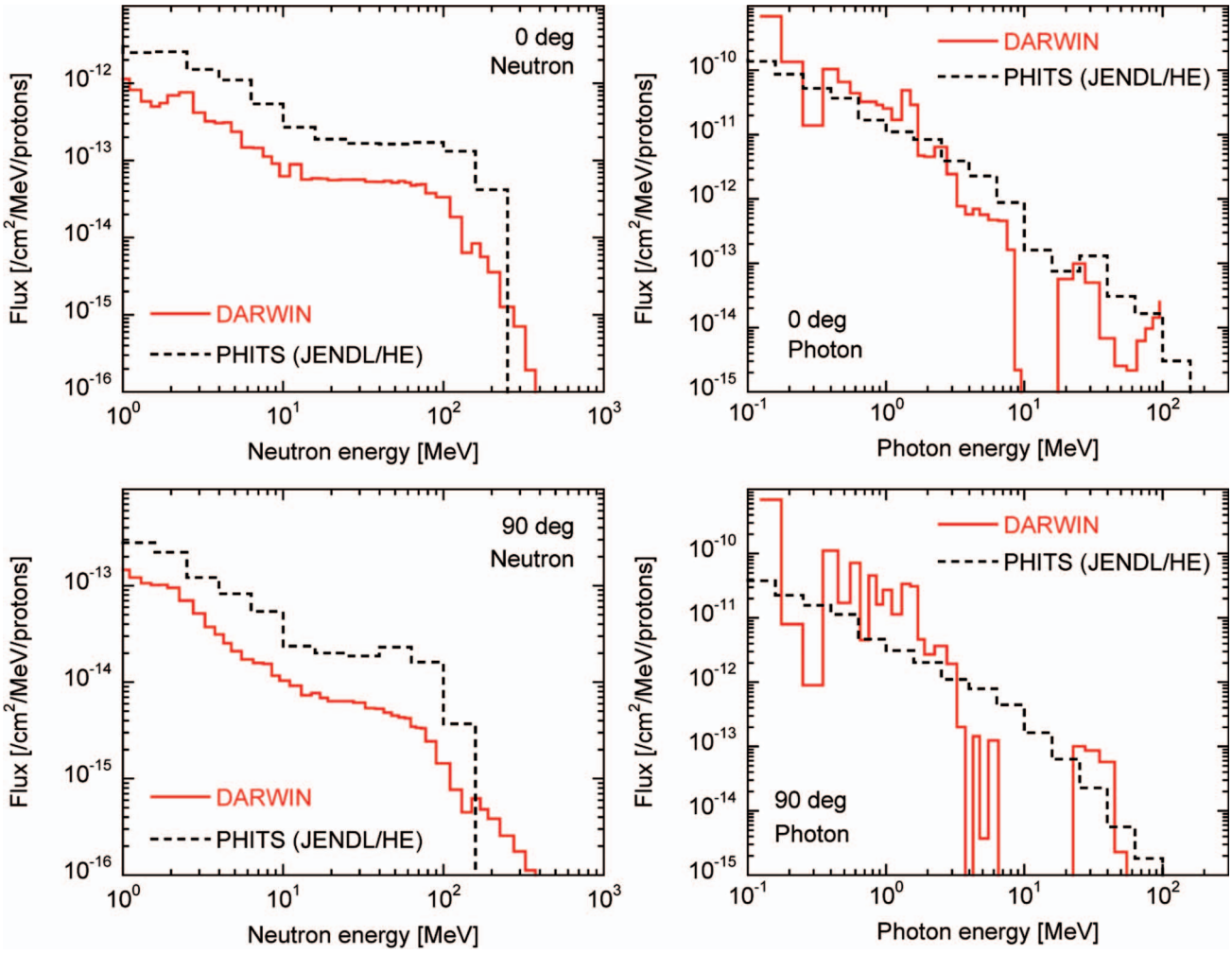

Figure 11. Energy spectra of neutrons and photons behind shields at 0° and 90°.

have an alternative approach for particle transport based on theoretical models. **Figure 12** depicts the neutron dose map around the water phantom calculated by PHITS with JENDL/HE (upper) and the hadronic cascade model, JAM (lower) [27]. From the figure, it is obvious that the contours of the dose rates are quite different between JENDL/HE and JAM at the forward region along the beam axis. This comes from the difference in neutron production yield by proton incident reaction in the JENDL/HE and JAM calculations. **Figure 13** presents the calculation results of neutron-production double-differential cross sections at 0°, 7.5°, 30°, and 60° from a carbon nucleus bombarded by 256-MeV protons, together with the experimental data obtained at LANL [28]. At forward angles, the spectrum has a peak structure located around the incident energy. The JENDL/HE forms the peak in the spectrum. Conversely, JAM fails to reproduce the peak structure, especially at 0°. The same tendency was observed in the JAM calculations for not only the carbon nucleus but also other nuclei such as oxygen constituting the water phantom. The lack of a high-energy neutron component in the forward spectra calculated by JAM results in underestimation of the neutron dose rates downstream of the water phantom as shown in Figure 12. Thus, we recommend that nuclear data files are used with PHITS in design calculations for facility shielding.

In general, it is very difficult for theoretical models to reproduce the neutron production at the most-forward angles because both the corrective motion of nucleons inside a nucleus and the Pauli exclusion principle affect the production of forward neutrons and are difficult for a model to contend with. The same situation exists for other theoretical models such as MCNPX, FLUKA, and GEANT4. Furthermore, experimental data at the most-forward angles applicable to the validation of theoretical models are very scarce [29,30]. The high-energy nuclear data file is also evaluated on the basis of the calculation results by theoretical models. Hence, reliable experimental data are urgently needed to improve the theoretical models and the sophistication of the nuclear data file.

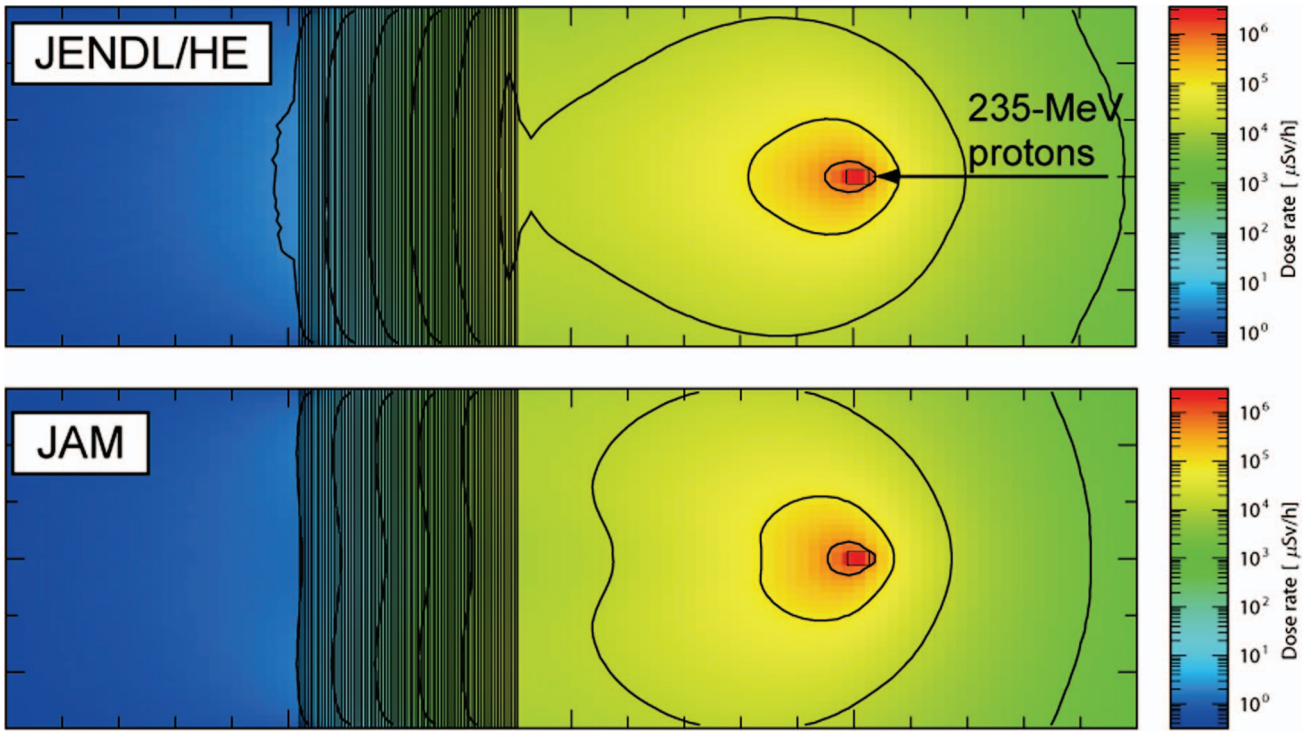

Figure 12. Neutron dose map around water phantom calculated by PHITS with JENDL/HE (upper) and JAM (lower).

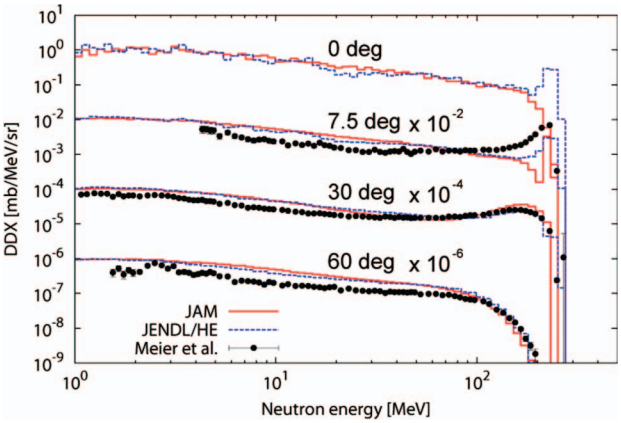

Figure 13. Neutron-production double-differential cross sections of carbon by 256-MeV protons. Solid and dashed curves indicate the calculation results by PHITS with JAM and JENDL/HE, respectively. Marks are experimental data obtained by Meier et al. at LANL [28].

6.2. *Maze*

Figure 14 compares neutron dose distributions in the maze between the experiment and the calculations. The horizontal axis indicates the distance from the mouth of the first leg along the centerline of the passage depicted in Figure 8 with a dotted line. Closed circles represent experimental data measured by the solid-state nuclear track detectors. Solid and dashed lines are the calculation results of the Monte Carlo code PHITS with JENDL/HE and the analytical model based on Nakamura and Uwamino's formulas [3] with the parameters used in the design planning, respectively. Open squares indicate the PHITS results for neutrons below 15 MeV. The dose rates given by the analytical model are described in effective dose, and those of the others are in ambient dose equivalent, H*(10). No data were measured at the farthest point in the third leg because the dose rate was under the detection limit.

With respect to the absolute values, the results of the experiment and calculations deviate from each other within one order. The experiment gives the lowest values, the analytical model is the highest, and PHITS is in the middle. As already mentioned above, the track detector has no sensitivity for high-energy (>15 MeV) neutrons [16]. The experimental data of the track detectors agree well with the results of PHITS for neutrons <15 MeV in the first leg, while PHITS gives slightly larger values in the subsequent legs. A hollow observed in the PHITS calculation for the first leg is caused by a shadow on the concrete wall beside the mouth of the maze, as depicted in Figure 8. As in the case of bulk shielding, the analytical model gives large values because the source term is overestimated.

The dose attenuation rates, which are derived by normalizing the dose rates at each location to the one at the mouth of the first leg, are shown in **Figure 15**. While the results of the experiment and calculations represent a similar attenuation curve, the slope of the attenuation rate by the analytical model differs from

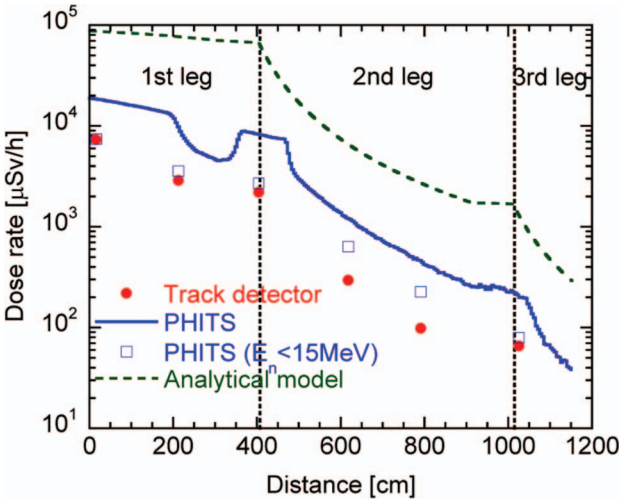

Figure 14. Neutron dose distribution in the maze. The horizontal axis indicates distance from the mouth of the first leg along the center of the passage.

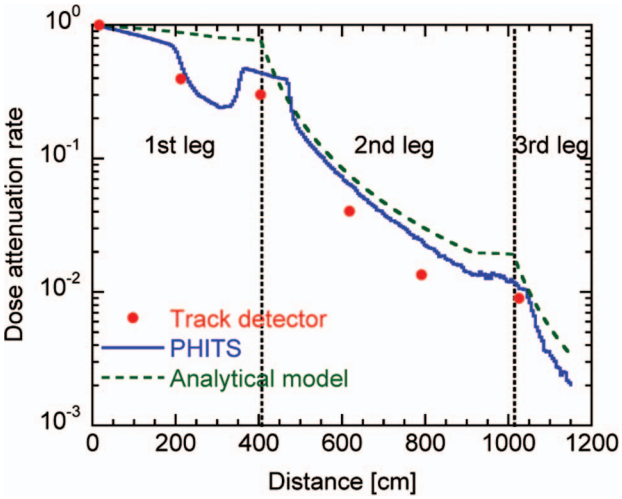

Figure 15. Neutron dose attenuation rate in the maze. The horizontal axis indicates distance from the mouth of the first leg along the center of the passage.

the others in the first leg. This comes from the assumption employed for a conservative estimation in the design planning; that is, 1.0 was used as the correction term A'/A in Equation (2) for source visibility from the mouth of the first leg. In the second and succeeding legs, the neutron dose rates would be reduced by decreasing the magnitude of the energy spectra without dramatically changing their shapes. The attenuation curves in those legs are reproduced well by an inverse square law.

In the maze calculations, the analytical model that used the parameter set from the facility design evaluated dose rates with a good margin of safety. The Monte Carlo code PHITS gives practical results that are smaller than those of the analytical model and are relatively close to the measured data.

7. Conclusion

Neutron dose values were measured behind the shields and at the maze of the Fukui Prefectural Hospital Proton Therapy Center in order to investigate the validity of both the analytical models used in facility design and the Monte Carlo code PHITS. While the values measured by DARWIN and Wendi-2 agreed well, the ordinary rem meter that has a limit of applicable energy around 17 MeV underestimated the neutron dose to about 40%. We insist that this underestimation should be minded in a radiation monitoring at high-energy accelerator facilities using rem meters.

The analytical models gave very conservative results compared with the other results obtained, because the source term of the model was estimated with a large margin of safety. On the basis of the results, we conclude that the Fukui Prefectural Hospital Proton Therapy Center, which was designed with analytical models, ensures sufficient radiation safety for workers and the public. This also means that the facility can potentially increase the patient workload without modifying the shielding.

The PHITS code predicted more realistic dose rates than those of the analytical models; that is, the values lay between those from the experiment and the analytical calculation. We therefore conclude that the use of Monte Carlo codes is currently the preferable method for estimating radiation safety at accelerator-based proton treatment facilities. However, problems in the shielding calculation by PHITS became apparent in the present study with respect to secondary particle production, especially the neutron yields in the most-forward direction. These problems would be solved by new experimental data to complement a systematic data set of particle production cross sections. Demand for charged particle radiotherapy is continuing to increase with the increasing population of cancer patients. A compact shielding optimized by Monte Carlo codes reduces the construction cost of a facility while maintaining radiation safety, making it feasible to locate such facilities near patients living in densely populated urban settings.

Acknowledgements

We are grateful to Dr. T. Sato and Dr. T. Fukahori for fruitful discussions with us on this study. We also acknowledge Drs. M. Hagiwara, H. Iwase, and Y. Iwamoto for their support in preparation of the experiment.

References

[1] Particle Therapy Co-Operative Group (PTCOG). Available at http://ptcog.web.psi.ch/ [website].
[2] Y. Makita, T. Nakamura, H. Tsuchidate, and M. Yamazaki, Radiation shielding design of a cancer therapy facility using compact proton synchrotron, *J. Nucl. Sci. Technol.* Supplement 4 (2004), pp. 18–21.

[3] T. Nakamura and Y. Uwamino, Shielding design and detection of neutrons from medical and industrial electron accelerators [in Japanese], *Radioisotopes* 35 (1986), pp. 51–56.

[4] K. Niita, N. Matsuda, Y. Iwamoto, H. Iwase, T. Sato, H. Nakashima, Y. Sakamoto, and L. Sihver, *PHITS: particle and heavy ion transport code system, version 2.23*, JAEA-Data/Code 2010-022, Japan Atomic Energy Agency (JAEA), 2010.

[5] D.B. Pelowitz (ed.), *MCNPX*^{TM} *user's manual*, LA-CP-11-00438, Los Alamos National Laboratory (LANL), 2011.

[6] A. Ferrari, P.R. Sala, A. Fassò, and J. Ranft, *Fluka: a multi-particle transport code (program version 2005)*, CERN-2005-10, European Organization for Nuclear Research (CERN), 2005.

[7] S. Agostinelli, J. Allison, K. Amako, et al., GEANT4 – a simulation toolkit, *Nucl. Instrum. Methods* 506 (2003), pp. 250–303.

[8] H. Nakashima, Y. Nakane, F. Masukawa, N. Matsuda, T. Oguri, H. Nakano, N. Sasamoto, T. Shibata, T. Suzuki, T. Miura, M. Numajiri, N. Nakao, H. Hirayama, and S. Sasaki, Radiation safety design for the J-PARC project, *Radiat. Prot. Dosimetry* 115 (2005), pp. 564–568.

[9] U. Titt and W.D. Newhauser, Neutron shielding calculations in a proton therapy facility based on Monte Carlo simulations and analytical models: criterion for selecting the method of choice, *Radiat. Prot. Dosimetry* 115 (2005), pp. 144–148.

[10] F. Stichelbaut, T. Canon, and Y. Jongen, Shielding studies for a hadron therapy center, *Nucl. Technol.* 168 (2009), pp. 477–481.

[11] T. Sato, D. Satoh, A. Endo, N. Shigyo, F. Watanabe, H. Sakurai, and Y. Arai, Upgrades of DARWIN, a dose and spectrum monitoring system applicable to various types of radiation over wide energy ranges, *Nucl. Instrum. Methods A* 637 (2011), pp. 149–157.

[12] T. Sato, D. Satoh, A. Endo, and Y. Yamaguchi, Development of dose monitoring system applicable to various radiations with wide energy ranges, *J. Nucl. Sci. Technol.* 42 (2005), pp. 768–778.

[13] R.H. Olsher, H. Hsu, A. Beverding, J.H. Kleck, W.H. Casson, D.G. Vasilik, and R.T. Devine, WENDI: an improved neutron rem meter, *Health Phys.* 79 (2000), pp. 170–181.

[14] R.H. Olsher and D.T. Seagraves, A ^{3}He counter version of the thermo fisher scientific NRD neutron rem meter, *Health Phys.* 94 (2008), pp. 71–74.

[15] *KWD Nuclear Instruments*. Available at http://www.kwdnuclearinstruments.se/ [website].

[16] H. Ohguchi and T. Nakamura, Development of wide-energy range personal neutron dosimeter using CR-39 track detector, *Appl. Radiat. Isot.* 46 (1995), pp. 509–510.

[17] M.M. Meier, W.B. Amian, C.A. Groulding, G.L. Morgan, and C.E. Moss, Neutron yields from stopping-length targets for 256-MeV protons, *Nucl. Sci. Eng.* 110 (1992), pp. 299–301.

[18] W.W. Engle, Jr., *A user's manual for ANISN: a one dimensional discrete ordinates transport code with anisotropic scattering*, K-1693, Oak Ridge National Laboratory (ORNL), 1973.

[19] R.G. Alsmiller, Jr., J.M. Barnes, and J.D. Drischler, *Neutron-production multigroup cross sections for neutron energies less than or equal to 400 MeV (revision 1)*, ORNL/TM-9801, Oak Ridge National Laboratory (ORNL), 1986.

[20] S. Moriuchi and I. Miyanaga, A spectrometric method for measurement of low-level gamma exposure dose, *Health Phys.* 12 (1966), pp. 541–551.

[21] Y. Oyama, K. Sekiyama, and H. Maekawa, Spectrum weight function method for in-situ fast neutron and gamma-ray response measurements in fusion integral experiments with an NE213 scintillation detector, *Fusion Technol.* 26 (1994), pp. 1098–1102.

[22] M. Reginatto and P. Goldhagen, MAXED, a computer code for maximum entropy deconvolution of multi-sphere neutron spectrometer data, *Health Phys.* 77 (1999), pp. 579–583.

[23] M. Reginatto, P. Goldhagen, and S. Neumann, Spectrum unfolding, sensitivity analysis and propagation of uncertainties with the maximum entropy deconvolution code MAXED, *Nucl. Instrum. Methods A* 476 (2002), pp. 242–246.

[24] International Commission on Radiological Protection (ICRP), Conversion coefficients for use in radiological protection against external radiation, *ICRP Publ.* 74 (1996).

[25] A.V. Sannikov and E.N. Savitskaya, Ambient dose equivalent conversion factors for high energy neutron based on the ICRP 60 recommendations, *Radiat. Prot. Dosim.* 70 (1997), pp. 383–386.

[26] Y. Watanabe, T. Fukahori, K. Kosako, N. Shigyo, T. Murata, N. Yamano, T. Hino, K. Maki, H. Nakashima, N. Odano, and S. Chiba, *Nuclear data evaluations for JENDL high-energy file*, AIP Conference Proceedings, September 26–October 1, 2004, Santa Fe, NM, 2005.

[27] Y. Nara, N. Otuka, A. Ohnishi, K. Niita, and S. Chiba, Relativistic nuclear collisions at 10A GeV energies from p + Be to Au + Au with the hadronic cascade model, *Phys. Rev.* C61 (1999), pp. 024901-1–024901-19.

[28] M.M. Meier, W.B. Amian, C.A. Goulding, G.L. Morgan, and C.E. Moss, Differential neutron production cross sections for 256-MeV protons, *Nucl. Sci. Eng.* 110 (1992), pp. 289–298.

[29] D. Satoh, N. Shigyo, K. Ishibashi, Y. Takayama, S. Ishimoto, Y. Iwamoto, H. Tenzo, T. Nakamoto, M. Numajiri, and S. Meigo, Neutron-production double-differential cross sections of iron and lead by 0.8 and 1.5 GeV protons in the most-forward direction, *J. Nucl. Sci. Technol.* 40 (2003), pp. 283–290.

[30] Y. Iwamoto, S. Taniguchi, N. Nakao, T. Itoga, H. Yashima, T. Nakamura, D. Satoh, Y. Nakane, H. Nakashima, Y. Kirihara, M. Hagiwara, H. Iwase, K. Oishi, A. Tamii, and K. Hatanaka, Measurement of thick target neutron yields at 0° bombarded with 140, 250 and 350 MeV protons, *Nucl. Instrum. Methods A* 593 (2008), pp. 298–306.